Calculations of ^{8}He+p elastic cross sections using a microscopic optical potential

V. K. Lukyanov,[1] E. V. Zemlyanaya,[1] K. V. Lukyanov,[1] D. N. Kadrev,[2] A. N. Antonov,[2] M. K. Gaidarov,[2] and S. E. Massen[3]
[1]*Joint Institute for Nuclear Research, Dubna RU-141980, Russia*
[2]*Institute for Nuclear Research and Nuclear Energy, Bulgarian Academy of Sciences, Sofia 1784, Bulgaria*
[3]*Department of Theoretical Physics, Aristotle University of Thessaloniki, 54124 Thessaloniki, Greece*
(Received 1 June 2009; published 27 August 2009)

An approach to calculate microscopic optical potential with the real part obtained by a folding procedure and with the imaginary part inherent in the high-energy approximation is applied to study the ^{8}He+p elastic-scattering data at energies of tens of MeV/nucleon. The neutron and proton density distributions obtained in different models for ^{8}He are used in the calculations of the differential cross sections. The role of the spin-orbit potential is studied. Comparison of the calculations with the available experimental data on the elastic-scattering differential cross sections at beam energies of 15.7, 26.25, 32, 66, and 73 MeV/nucleon is performed. The problem of the ambiguities of the depths of each component of the optical potential is considered by means of the imposed physical criterion related to the known behavior of the volume integrals as functions of the incident energy. It is shown also that the role of the surface absorption is rather important, in particular for the lowest incident energies (e.g., 15.7 and 26.25 MeV/nucleon).

DOI: 10.1103/PhysRevC.80.024609 PACS number(s): 24.10.Ht, 25.60.−t, 21.30.−x, 21.10.Gv

I. INTRODUCTION

The experiments with intensive secondary radioactive nuclear beams have made it possible to investigate the structure of light nuclei near the neutron and proton drip lines as well as the mechanism of scattering of the weakly bound nuclei. Special attention has been paid to the neutron-rich isotopes of helium (^{6,8}He), lithium (^{11}Li), berilium (^{14}Be), and others, in which several neutrons are situated in the far extended nuclear periphery and form a "halo." A widely used way to study the structure of exotic nuclei is to analyze their elastic scattering on protons or nuclear targets at different energies. Here we would like to mention, for example, the experiments on scattering of helium isotopes on protons at incident energies $E_{\rm inc}$ less than 100 MeV/nucleon, namely for ^{6}He at energy 25.2 [1–5], 38.3 [6], 41.6 [7–9], and 71 MeV/nucleon [10,11], for ^{8}He at energy 15.7 [12], 26 [3], 32 [10,11], 66 [10,11], and 73 MeV/nucleon [10,11,13], also at energy 700 MeV/nucleon for He and Li isotopes (e.g., Refs. [14–18]).

The experimental data on differential and total reaction cross sections of processes with light exotic nuclei have been analyzed using a variety of phenomenological and microscopic methods (e.g., Refs. [10,11,14–40]). Among the latter methods we note, e.g., the microscopic analysis based on the coordinate-space g-matrix folding method [25–32], as well as works where the real part of optical potential (OP) is microscopically calculated using the folding approach (e.g., Refs. [22–26,40–45]). Usually the imaginary part of the OP's and the spin-orbit (SO) terms have been determined phenomenologically. Thus, the OP's have a number of fitting parameters. For example, OP's have been used to elaborate the elastic differential cross sections of ^{6}He+p, ^{6}He+^{4}He ($E_{\rm inc}$ = 25 MeV/nucleon) [22], and ^{6}He+p and ^{8}He+p ($E_{\rm inc}$ < 100 MeV/nucleon) [23] by means of the M3Y-Paris effective NN interaction [42,43,46]. In the calculations the proton and neutron densities of the helium isotopes obtained by Tanihata *et al.* [47] and also in the cluster-orbital shell-model approximation (COSMA) [10,11,20,21] were applied. It was shown [23] that the elastic scattering is sensitive to different density distributions used in the folding approach.

In our previous work [40] to exclude the usage of the phenomenological imaginary part of OP we have performed calculations of ^{6}He+p elastic differential cross sections by means of the microscopic OP with the imaginary part taken from the OP derived in Refs. [48,49] on the basis of the high-energy approximation (HEA) [50–52]. This method (Glauber approach) in its optical limit [52] makes it possible to obtain an analytic expression of the scattering amplitude with the eikonal phase in the form of the so-called profile function. The latter is proportional to the integral of the one-particle density distributions of the colliding systems, and the integration is performed along a straight-line trajectory of motion. Generally, the integral contains also the form factor of the NN scattering amplitude and thus its form is akin to that of the standard folding potential with the NN potential instead of the NN amplitude. The NN amplitude itself is known from the experimental data and, therefore, the usage of a profile function offers certain advantages over approaches based on the folding potential. So, in nuclear physics, the HEA amplitude is applied to energies larger than 100 MeV/nucleon (see, e.g., Refs. [14,53,54]). However, in the past two decades the HEA was generalized and applied to lower energies. The prescription to calculate the profile function consists in a replacement of the straight-line trajectory impact parameter b by the distance of closest approach r_c in the Coulomb field or by the respective distance r_{cn} in the presence of the nuclear field (real part of OP). By doing so, a reasonable agreement with the experimental data on the proton- and nucleus-nucleus reaction cross sections has been obtained in the region of energies from 10 to 1000 MeV/nucleon (see, e.g., Refs. [48,49,55–60]). However, this approach becomes fairly rough when one calculates differential cross sections and also the total cross sections at comparably low energies. Moreover, in the case of the microscopic OP given in a form

of tables, this approach needs a numerical solution of the classical equation of motion to get the corresponding trajectory of motion. For this reason the method is not efficient for applications because of quite complicated calculations. In this case the better way is to explore the equivalent HEA optical potential outlined in [48,49] and then to solve the respective Schrödinger equation numerically using a standard code that enables one to get the exact scattering amplitude and the total reaction cross sections, including the interference terms.

We used this approach in Ref. [40] to get the microscopic HEA imaginary part of the OP (ImOP) and added the real part of OP (ReOP) [41,42]. The ReOP includes the direct term and the exchange one that involves nonlinearity effects. Also, the role of the spin-orbit interaction has been considered. Additionally, the density dependence of the effective NN interaction, as well as the sensitivity of the results to the predictions of different theoretical models for the density of ^{6}He have been studied. It was shown that the more sophisticated large-scale shell model (LSSM) [44,45] density of ^{6}He is the most preferable one because it has led to a better agreement with the data. It was concluded in Ref. [40] that the use of the microscopic folding ReOP (V^F) and the HEA ImOP (W^H) has led to agreement with the data on ^{6}He+p elastic-scattering cross sections for 41.6 and 71 MeV/nucleon. However, the data at lowest energy 25.2 MeV/nucleon have been explained only on a qualitative level that is related to the limitations of using the HEA ImOP for energies around and less than 25 MeV/nucleon. This has led to the necessity to reduce strongly the depth of HEA ImOP. It was shown in Ref. [40] that the OP in the form $U_{\rm opt} = N_R V^F + i N_I W^H$ with both V^F and W^H calculated microscopically and using only two free parameters N_R and N_I that renormalize the ReOP and ImOP depths can be reasonably applied to calculations of scattering cross sections at energies $E_{\rm inc} < 100$ MeV/nucleon, such as 41.6 and 71 MeV/nucleon.

In the present work we apply the developed approach to study the existing experimental data on ^{8}He+p elastic scattering cross sections at incident energies less than 100 MeV/nucleon. Various model densities of ^{8}He, such as those obtained within the approach of Tanihata *et al.* [47], LSSM [44,45], and the Jastrow correlation method (JCM) [61,62], are used to calculate the OP's. We study the role of the spin-orbit terms and, in addition to our previous study [40], we consider two more parameters, $N_R^{\rm SO}$ and $N_I^{\rm SO}$ (when necessary), that renormalize the depths of the real and imaginary parts of the SO potential, respectively. In addition, the nuclear surface effects are also studied by introducing an additional surface term in OP. This is related to investigations of the lowest energy limit of the applicability of the HEA OP in ^{8}He+p elastic scattering. Also we pay attention to the energy dependence of the parameters N_R and N_I as well as to the respective volume integrals. We note the necessity to analyze the differential cross sections estimating simultaneously the values of the total reaction cross section. This would give an additional test of the various ingredients of the approach.

The theoretical scheme to calculate microscopically the real and imaginary parts of the OP, as well as the spin-orbit term, is given in Sec. II. The results of the calculations of OP's and elastic-scattering differential cross sections, including those from some methodical ones, and their discussion are given in Sec. III. The summary of the work and conclusions of the results are presented in Sec. IV.

II. THEORETICAL SCHEME

A. Direct and exchange parts of the real OP (ReOP)

Here we give briefly the main expressions for the real part of the nucleon-nucleus OP that is assumed to be a result of a single folding of the effective NN potential and the nuclear densities. It involves the direct and exchange parts (for more details, see, e.g., Refs. [41–43] and also [40]):

$$V^F(r) = V^D(r) + V^{EX}(r). \tag{1}$$

In Eq. (1) the direct part (V^D) is composed of the isoscalar (IS) and isovector (IV) contributrions, correspondingly:

$$V^D_{\rm IS}(r) = \int \rho_2(\mathbf{r}_2) g(E) F(\rho_2) v^D_{00}(s) d\mathbf{r}_2, \tag{2}$$

$$V^D_{\rm IV}(r) = \int \delta\rho_2(\mathbf{r}_2) g(E) F(\rho_2) v^D_{01}(s) d\mathbf{r}_2, \tag{3}$$

where $\mathbf{s} = \mathbf{r} + \mathbf{r}_2$,

$$\rho_2(\mathbf{r}_2) = \rho_{2,p}(\mathbf{r}_{2,p}) + \rho_{2,n}(\mathbf{r}_{2,n}), \tag{4}$$

$$\delta\rho_2(\mathbf{r}_2) = \rho_{2,p}(\mathbf{r}_{2,p}) - \rho_{2,n}(\mathbf{r}_{2,n}). \tag{5}$$

In Eqs. (4) and (5) $\rho_{2,p}(\mathbf{r}_{2,p})$ and $\rho_{2,n}(\mathbf{r}_{2,n})$ are the proton and neutron densities of the target nucleus. In Eqs. (2) and (3) the energy dependence of the effective NN interaction is taken in the usually used form:

$$g(E) = 1 - 0.003E. \tag{6}$$

Also, for the NN potentials v^D_{00} and v^D_{01} we use the expression from Ref. [43] for the CDM3Y6 type of the effective interaction based on the solution of the equation for the g matrix, in which the Paris NN potential has been used. The density dependence of the effective interaction is taken in the following form:

$$F(\rho) = C[1 + \alpha e^{-\beta\rho(\mathbf{r})} - \gamma\rho(\mathbf{r})], \tag{7}$$

where $C = 0.2658$, $\alpha = 3.8033$, $\beta = 1.4099$ fm^3, and $\gamma = 4.0$ fm^3.

The isoscalar part of the exchange contribution to the ReOP has the form (see, e.g., Ref. [40]):

$$V^{EX}_{\rm IS}(r) = g(E) \int \rho_2(\mathbf{r}_2, \mathbf{r}_2 - \mathbf{s}) F\left[\rho_2\left(\mathbf{r}_2 - \frac{\mathbf{s}}{2}\right)\right] \times v^{EX}_{00}(s) j_0[k(r)s] d\mathbf{r}_2, \tag{8}$$

where the density matrix $\rho_2(\mathbf{r}_2, \mathbf{r}_2 - \mathbf{s})$ is usually approximated by the expression:

$$\rho_2(\mathbf{r}_2, \mathbf{r}_2 - \mathbf{s}) \simeq \rho_2\left(\left|\mathbf{r}_2 - \frac{\mathbf{s}}{2}\right|\right) \hat{j}_1\left[k_{F,2}\left(\left|\mathbf{r}_2 - \frac{\mathbf{s}}{2}\right|\right) \cdot s\right] \tag{9}$$

with

$$\hat{j}_1(x) = \frac{3}{x} j_1(x) = \frac{3}{x^3}(\sin x - x\cos x) \tag{10}$$

and $v^{EX}_{00}(s)$ is the isoscalar part of the exchange contribution to the effective NN interaction. The local momentum $k(r)$ of

the incident nucleon in the field of the Coulomb and nuclear potential (ReOP) is [63]:

$$k^2(r) = \left(\frac{2m}{\hbar^2}\right)[E_{\rm c.m.} - V_c(r) - V(r)]\left(\frac{1+A_2}{A_2}\right). \quad (11)$$

Substituting Eq. (11) in Eq. (8) the iteration procedure was used to get the final result for the folding potential. One can see that in this procedure the required microscopic potential $V(r)$ [that has to be calculated according to Eq. (1)] appears in the expression for $k^2(r)$ [Eq. (11)] and, correspondingly, in the integrand of the integral in Eq. (8), i.e., in the expression for the exchange contribution to the OP. Thus, nonlinearity effects occur as typical ingredients of the model and they have to be taken carefully into account. In our consideration, for the highest energy (73 MeV/nucleon) 8 iterations and for the lowest one (15.7 MeV/nucleon) 13 iterations were large enough in the calculations of the folding potentials.

In Eq. (9) $k_{F,2}$ is the average relative momentum of a nucleon in a nucleus [63,64]:

$$k_{F,2}(r) = \left\{\frac{5}{3\rho}\left[\tau(\rho) - \frac{1}{4}\nabla^2\rho(r)\right]\right\}^{1/2}, \quad (12)$$

where we choose for the kinetic energy density $\tau(\rho)$ the expression from the extended Thomas-Fermi approximation [65,66]:

$$\frac{\tau(\rho)}{2} \simeq \tau_q(\rho_q) = \frac{3}{5}(3\pi^2)^{2/3}[\rho_q(r)]^{5/3} + \frac{|\nabla\rho_q(r)|^2}{36\rho_q(r)} + \frac{\nabla^2\rho_q(r)}{3} \quad (13)$$

valid for each kind of particles $q = n, p$. It is shown in Ref. [40] how the isovector part of the exchange ReOP can be obtained.

B. Density distributions of ^{8}He

In the calculations of the OP's we use the following point-nucleon density distributions of ^{8}He:

(i) The Tanihata densities deduced in Ref. [47] by means of comparison of the measured total reaction cross section of ^{6,8}He+^{12}C at 800A MeV with the respective expression from [67] derived in the framework of the optical limit of the Glauber theory:

$$\rho^X_{\rm point} = \frac{2}{\pi^{3/2}}\left\{\frac{1}{a^3}\exp\left[-\left(\frac{r}{a}\right)^2\right] + \frac{1}{b^3}\frac{(X-2)}{3}\left(\frac{r}{b}\right)^2\exp\left[-\left(\frac{r}{b}\right)^2\right]\right\}. \quad (14)$$

Here $X = Z, N$ and the parameter values of a and b can be determined from

$$a^2 = a^{*2}\left(1 - \frac{1}{A}\right), \quad b^2 = b^{*2}\left(1 - \frac{1}{A}\right), \quad (15)$$

where $a^* = 1.53$ fm and $b^* = 2.06$ fm; hence $a = 1.43$ fm and $b = 1.93$ fm for ^{8}He. So, the proton distribution is defined by the first term only, while an excess of neutrons is described by the additional second term. The rms radii of the point-proton and point-neutron densities of ^{8}He are equal to 1.76 and 2.69 fm, correspondingly;

(ii) The LSSM densities calculated in a complex $4\hbar\omega$ shell-model space [44,45] using the Woods-Saxon (WS) basis of single-particle wave functions with realistic exponential asymptotic behavior;

(iii) The densities obtained in Refs. [61,62] with accounting for the NN central-type short-range Jastrow correlations.

C. Optical potential within the high-energy approximation

In Ref. [40] the so-called complex HEA optical potential has been applied to explain the available data on the ^{6}He+p elastic differential cross sections and energies less than 100 MeV/nucleon. The HEA OP was derived in Ref. [48] on the basis of the eikonal phase inherent in the optical limit of the Glauber theory. Then, by means of this potential or taking only its imaginary part together with the folding real part of OP, the cross sections were calculated using the code DWUCK4 [68] for solving the Schrödinger equation. Thus, we do not apply the Glauber theory for calculating the scattering amplitude at relatively low energies but use the equivalent HEA OP to solve numerically the respective wave equation. In this case, the use of the ordinary Glauber theory leads to insuperable problems in performing integration in the eikonal phase mentioned in the Introduction. Indeed, there one should take into account the distortion of the integration path along classical trajectories in the field of the Coulomb and nuclear potentials (see, e.g., Refs. [48,55–60]). At the same time, to calculate the HEA OP one can use the definition of the eikonal phase as an integral of the nucleon-nucleus potential over the trajectory of the straight-line propagation, and have to compare it with the corresponding Glauber expression for the phase in the optical limit approximation. Doing so, the HEA OP can be obtained as a folding of form factors of the nuclear density and the NN amplitude $f_{NN}(q)$ [48,49]:

$$U^H_{\rm opt} = V^H + iW^H = -\frac{\hbar v}{(2\pi)^2}(\bar\alpha_{NN} + i)\bar\sigma_{NN} \times \int_0^\infty dq q^2 j_0(qr)\rho_2(q) f_{NN}(q). \quad (16)$$

In Ref. (16) $\bar\sigma_{NN}$ and $\bar\alpha_{NN}$ are, respectively, the NN total scattering cross section and the ratio of the real to imaginary parts of the forward NN scattering amplitude both averaged over the isospin of the nucleus. They both have been parametrized in Refs. [57,69] as functions of energies in a wide range from 10 MeV to 1 GeV and also at energies lower than 10 MeV. The values of these quantities can also account for the in-medium effect by a factor from Ref. [70].

D. The spin-orbit term

Following Refs. [68,71,72] the expression for the spin-orbit contribution to the OP can be written in the form:

$$V_{\rm LS}(r) = 2\lambda_\pi^2\left[V_0\frac{1}{r}\frac{df_R(r)}{dr} + iW_0\frac{1}{r}\frac{df_I(r)}{dr}\right](\mathbf{l}\cdot\mathbf{s}), \quad (17)$$

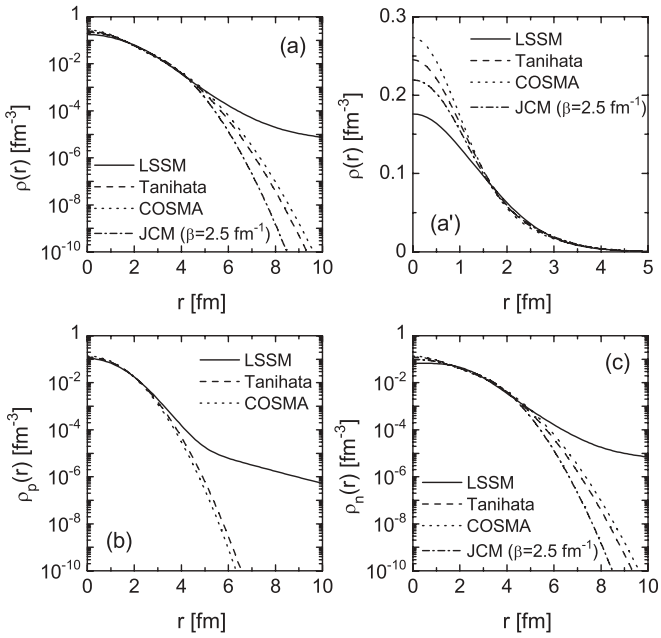

FIG. 1. Total [(a) and (a′)], point-proton (b), and point-neutron (c) densities of ^{8}He from the model of Tanihata [47], COSMA [20,21], LSSM [44,45], and JCM calculations [61,62].

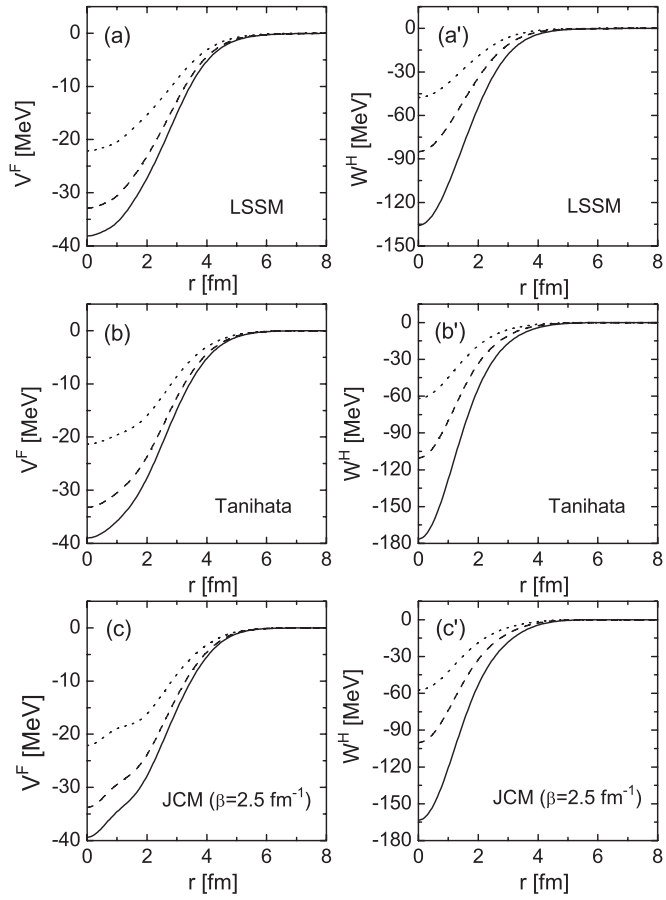

FIG. 2. Microscopic real part (V^F) of OP [(a), (b), and (c)] and HEA imaginary part (W^H) [(a′), (b′), and (c′)] calculated using the LSSM, Tanihata, and JCM ($\beta = 2.5$ fm^{-1}) densities of ^{8}He for energies $E = 15.7$ (solid lines), 32 (dashed lines), and 73 MeV/nucleon (dotted lines).

where $\lambda_\pi^2 = 2$ fm^2 is the squared pion Compton wavelength, V_0 and W_0 are the real and imaginary parts of the microscopic OP at $r = 0$, and $f(r)$ is the form of the real [$f_R(r)$] and imaginary [$f_I(r)$] parts of the microscopic OP taken as WS forms $f(r, R_R, a_R)$ and $f(r, R_I, a_I)$. In our calculations the parameters [half-radius $R_R(R_I)$ and diffuseness $a_R(a_I)$] are obtained by fitting the WS potential to the microscopically calculated real and imaginary contributions to the OP $V(r)$ and $W(r)$.

III. RESULTS AND DISCUSSION

In this section we present the results of the calculations of the microscopic OP's and the respective ^{8}He+p elastic scattering differential cross sections at energies $E_{\rm inc} <$ 100 MeV/nucleon. In principle, the OP's do not contain free parameters, but they depend on the density distribution of the target nucleus. This allows one to test advanced theoretical methods that give predictions for the density distribution. In the case of ^{8}He we used the semiempirical model of Tanihata [47], the large-scale shell model [44,45], as well as the results of the approach [61,62] within the JCM. In Fig. 1 in logarithmic and linear scales are shown the proton $\rho_p(r)$, neutron $\rho_n(r)$, and matter $\rho(r)$ densities of ^{8}He obtained in different models. Also, for comparison, the known COSMA densities [20,21] are presented. We note that among them only the LSSM densities have a realistic exponential asymptotics, whereas the others have a Gaussian one. The results for the JCM densities are given for the value of the correlation parameter $\beta = 2.5$ fm^{-1} in the Jastrow correlation factor $1 - e^{-\beta^2 r^2}$, where r is the distance between neutrons. It was shown in Refs. [61,62] that the inclusion of this factor causes a slight increase of the density in the central part of the nucleus. Simultaneously, as can be seen in Fig. 2, this leads to a small decrease of the depth of the imaginary part of OP in comparison with the case of the Tanihata density. In the same figure we show as examples the real V^F and imaginary W^H parts of the ^{8}He+p OP's for energies 15.7, 32, and 73 MeV/nucleon calculated using different densities. V^F is calculated by a folding procedure and W^H within the HEA (see Sec. II). It is seen that the increase of the energy leads to reduced depths and slopes of ReOP and ImOP.

We calculated the ^{8}He+p elastic scattering differential cross sections using the program DWUCK4 [68] and using the microscopically obtained real V^F and imaginary W^H contributions to the optical potential:

$$U_{\rm opt}(r) = N_R V^F(r) + i N_I W^H(r) + 2\lambda_\pi^2 \left\{ N_R^{\rm SO} V_0^F \frac{1}{r}\frac{df_R(r)}{dr} + i N_I^{\rm SO} W_0^H \frac{1}{r}\frac{df_I(r)}{dr} \right\} (\mathbf{l}\cdot\mathbf{s}), \quad (18)$$

where V_0^F and W_0^H are the depths of the SO optical potential obtained simultaneously with $R_R(R_I)$ and $a_R(a_I)$ from the

approximation of the volume real and imaginary OP's by Woods-Saxon form.

So, further in the present work we consider the set of the N coefficients as parameters to be found out from comparisons with the experimental data. We consider such a model as the appropriate physical basis, which constraints the fitting procedure by the established model forms of searching potentials. We emphasize here that in our work we do not aim to find perfect agreement with the empirical data. In this sense, the introduction of the fitting parameters (N's) related to the depths of the different components of the OP's can be considered as a way to introduce a quantitative measure of the deviations of the predictions of our approach from the reality (e.g., the differences of N's from unity for given energies, as can be seen below).

The discussion that follows is based on the fitting procedure, where the additionally introduced strength parameters N_R, N_I, $N_R^{\rm SO}$, $N_I^{\rm SO}$ are varied step by step. So, we start from the case $N_R = N_I = 1$, $N_R^{\rm SO} = N_I^{\rm SO} = 0$, then fit successively both coefficients N_R and N_I, and after that the values of $N_R^{\rm SO}$ and $N_I^{\rm SO}$. First, we give in Fig. 3 the results of our methodical calculations of the cross sections for different energies (15.7, 26, 32, 66, and 73 MeV/nucleon) using the densities of ^{8}He from LSSM, Tanihata, and JCM approaches in the case when $N_R = N_I = 1$ and $N_R^{\rm SO} = N_I^{\rm SO} = 0$ (i.e., without spin-orbit interaction). It can be seen that the behavior of the cross sections for a given energy and interval of angles is weakly sensitive to the choice of the model for the density of ^{8}He. In spite of this uncertainty we choose for the further applications the LSSM density because it has a realistic exponential behavior in the peripheral region of the nucleus.

The second methodical study is a test of the effect of Jastrow central short-range NN correlations on mechanism of the considered process of scattering. As known, the main parameter that governs the contribution of these correlations is β, and we change it in wide limits from 2.5 to 50 fm^{-1}. It is seen in Fig. 4 that these changes result in an increase of the neutron density of about 2.5 times in the central part of ^{8}He but this has no important effect on the calculated OP's and on the shape of the respective differential cross sections. Therefore, in the further calculations we do not account for the short-range correlation effects.

Later, as a next step, we allow the "depth" of each of the parts of the OP (18) in our semimicroscopic models to vary to find the optimal values of the parameters N_R, N_I, $N_R^{\rm SO}$,

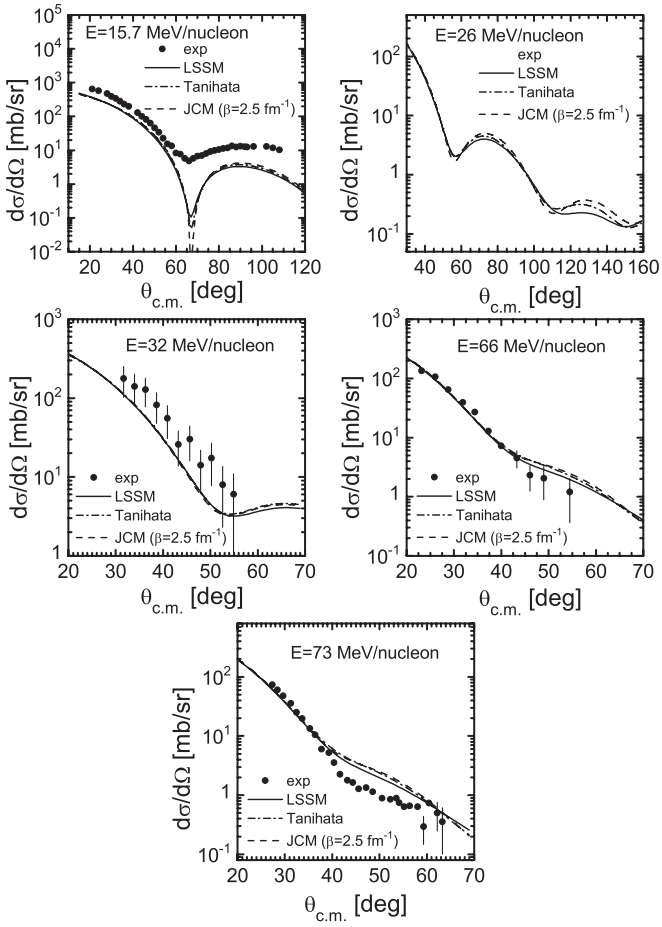

FIG. 3. The ^{8}He+p elastic-scattering cross sections at different energies calculated using $U_{\rm opt}$ [Eq. (18)] for values of the parameters $N_R = N_I = 1$ and $N_R^{\rm SO} = N_I^{\rm SO} = 0$. The used densities of ^{8}He are LSSM (solid line), Tanihata (dash-dotted line), and JCM ($\beta = 2.5$ fm^{-1}) (dashed line). Experimental data are taken for 15.7 [12], 26 [3], 32 [10,11], 66 [10,11], and 73 MeV/nucleon [10,11,13].

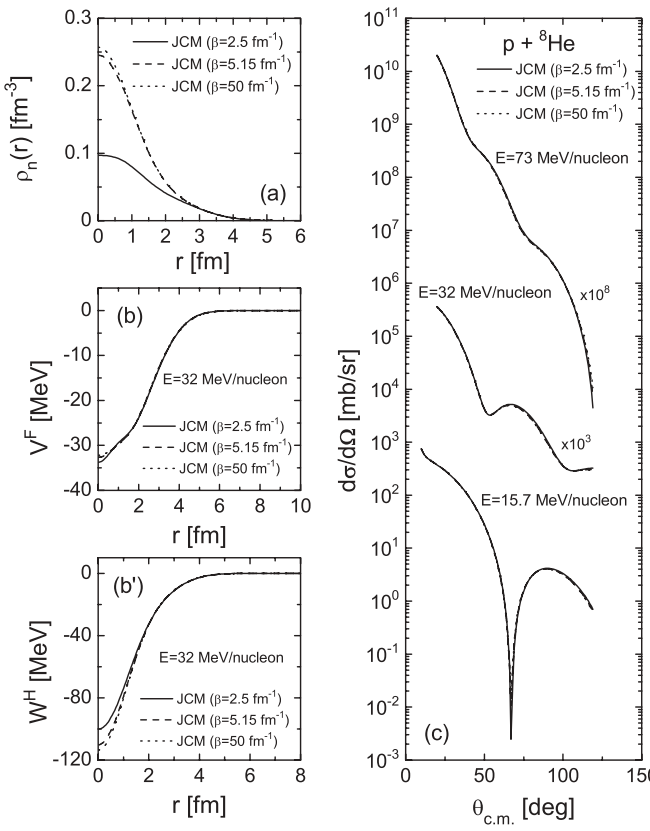

FIG. 4. Point-neutron density of ^{8}He (a), V^F and W^H of OP [(b) and (b′)] for energy $E = 32$ MeV/nucleon, and ^{8}He+p elastic-scattering cross sections (c) at energies $E = 15.7, 32$, and 73 MeV/nucleon calculated using JCM densities of ^{8}He for three values of the correlation parameter β.

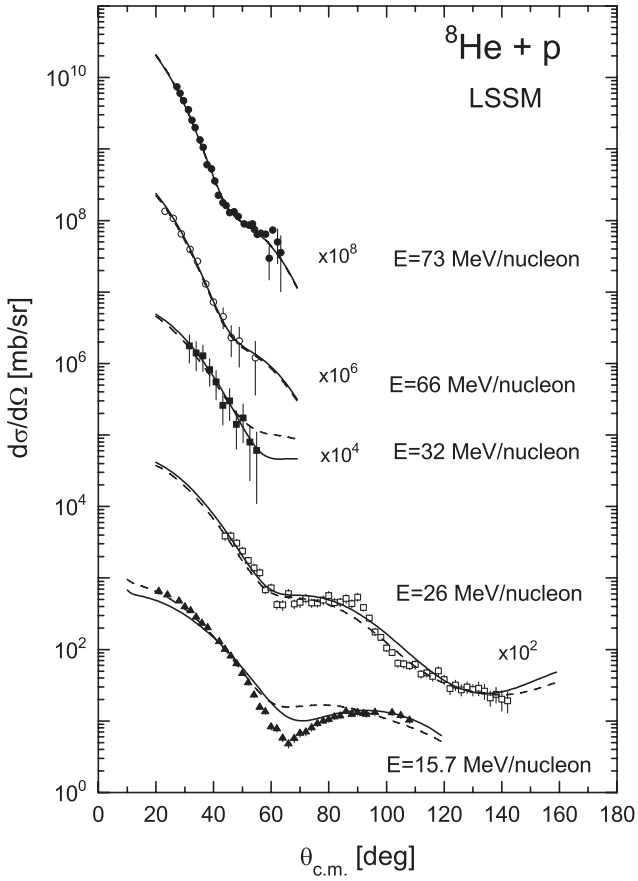

FIG. 5. The ^{8}He+p elastic-scattering cross sections at different energies calculated using $U_{\rm opt}$ [Eq. (18)] for various values of the renormalization parameters N_R, N_I, $N_R^{\rm SO}$, and $N_I^{\rm SO}$ (presented in Table I) giving the best agreement with the data. The used density of ^{8}He is LSSM. Experimental data are taken for 15.7 [12], 26 [3], 32 [10,11], 66 [10,11], and 73 MeV/nucleon [10,11,13].

and $N_I^{\rm SO}$ by a fitting procedure to the available experimental data for the cross sections. In Fig. 5 we present the results of our calculations of ^{8}He+p elastic scattering cross sections for various energies and the LSSM density with the fitted values of the parameters N_R, N_I, $N_R^{\rm SO}$, and $N_I^{\rm SO}$. The values of these renormalization parameters are given in Table I together with the predicted total reaction cross sections. The results obtained using the values of the parameters from the first line of this table for each energy are given by solid line in Fig. 5, while those from the second line for each energy are given by dashed line.

As is known, however, the problem of the ambiguity of the values of the parameters N arises when the fitting procedure is applied to a limited number of experimental data. For instance, in the case of the LSSM density, the values of $N_R = 1.0$ and 0.9, and correspondingly $N_I = 0.236$ and 0.1 (with $N_R^{\rm SO} = 0.107$ and $N_I^{\rm SO} = 0.040$) lead to similar results in the case of 15.7 MeV/nucleon. For $E = 32$ MeV/nucleon the results are similar when $N_R = 1.0$, $N_I = 0.374$ and $N_R = 0.438$, $N_I = 0.036$; for $E = 66$ MeV/nucleon the results are similar when $N_R = 0.876$, $N_I = 0.071$ and $N_R = 0.854$, $N_I = 0.086$; for $E = 73$ MeV/nucleon they are similar when $N_R = 0.875$, $N_I = 0.020$; $N_R = 0.869$, $N_I = 0.010$ (with $N_R^{\rm SO} = 0.009$ and $N_I^{\rm SO} = 0.002$). Our calculations produce similar results when using the Tanihata density. We note that in some cases it has been enough to vary only the volume part of the OP, i.e., the values of the parameters N_R and N_I without the spin-orbit parts of the OP. When all four parameters N are fitted the results for a given energy are similar, as already mentioned above. Thus, the problem to choose the most physical values of the parameters N arises. It is known that because the procedure of fitting belongs to the class of the ill-posed problems (see, e.g., Ref. [73]), it is necessary to impose some physical constraints on the choice of the set of parameters N. One of them is the total cross section of scattering and reaction. However, the corresponding values are missing at the energy interval considered in our work. To our knowledge, the total reaction cross section σ_R of ^{8}He+p process is known only at energy 670 MeV and it is about 200 mb [14].

TABLE I. The renormalization parameters N_R, N_I, $N_R^{\rm SO}$, and $N_I^{\rm SO}$ obtained by fitting the experimental data in Fig. 5 in the case of LSSM density. The energies are in MeV/nucleon and the total reaction cross sections σ_R are in mb.

E	N_R	N_I	$N_R^{\rm SO}$	$N_I^{\rm SO}$	σ_R
15.7	1.0	0.236	0	0	603.6
15.7	0.9	0.1	0.107	0.040	693
26	0.422	0.104	0.090	0.010	275.11
26	0.439	0.144	0.087	0.023	377.22
32	0.438	0.036	0.096	0	71.9
32	1.0	0.374	0	0	419.5
66	0.876	0.071	0	0	55.7
66	0.854	0.086	0	0	65.9
73	0.875	0.02	0	0	1.48
73	0.869	0.01	0.010	0.002	1.22

Another physical criterion that has to be imposed on the choice of the values of the parameters N is the behavior of the volume integrals [41]

$$J_V = \frac{4\pi}{A}\int drr^2[N_R V^F(r)], \tag{19}$$

$$J_W = \frac{4\pi}{A}\int drr^2[N_I W^H(r)] \tag{20}$$

as functions of the energy.

It has been pointed out (see, e.g., Romanovsky *et al.* [74] and references therein) that the values of the volume integral J_V decrease with the increase of the energy in the interval $0 < E < 100$ MeV/nucleon, while J_W is almost constant in the same interval. Imposing this behavior of J_V and J_W on our OP's (i.e., on their "depth" parameters N_R and N_I), we obtain by the fitting procedure the values of the parameters given in Table II.

The results of the calculations of the cross sections are presented in Fig. 6 for the case of the LSSM density together with the volume integrals J_V and J_W as functions of the energy. The results obtained using the values of the parameters from the first line of Table II for the energies 15.7 and 73 MeV/nucleon are given by solid line in Fig. 6(a), while

TABLE II. The parameters N_R, N_I, N_R^{SO}, and N_I^{SO}, the volume integrals J_V and J_W (in MeV fm^3) as functions of the energy E (in MeV/nucleon) [selected in correspondence to the behavior shown in Figs. 6(b) and 6(c)], and the total reaction cross sections σ_R (in mb) for the ^{8}He+p scattering in the case of LSSM density [the results of the fit are shown in Fig. 6(a)].

E	N_R	N_I	N_R^{SO}	N_I^{SO}	J_V	J_W	σ_R
15.7	0.630	0.064	0.139	0.070	411.1	58.6	722.0
15.7	0.630	0.052	0.166	0.057	411.1	47.6	701.2
26	0.644	0.128	0.035	0.026	377.7	84.35	381.2
32	0.648	0.120	0.062	0.022	358.3	69	302.7
66	0.852	0.131	0	0	344.2	45	95.2
73	0.869	0.090	0.004	0	330.0	29	60.9
73	0.869	0.063	0.010	0	330.0	20.25	43.9

those from the second line for these energies are given by dashed line. In comparison to the data in Table I one can see that the total reaction cross sections decrease monotonically with the energy increased. Also, we reach the smooth change of the values of the volume integrals with the energy increase. Moreover, with the energy increase one sees the monotonic increase of the renormalization coefficients N_R of the volume real part of OP together with an "average" decreasing of N_I inherent in the imaginary part of OP. Almost a regular behavior is obtained for the spin-orbit correction coefficients N_R^{SO} and N_I^{SO}. So, the N_R coefficient is going to 1 in coincidence with

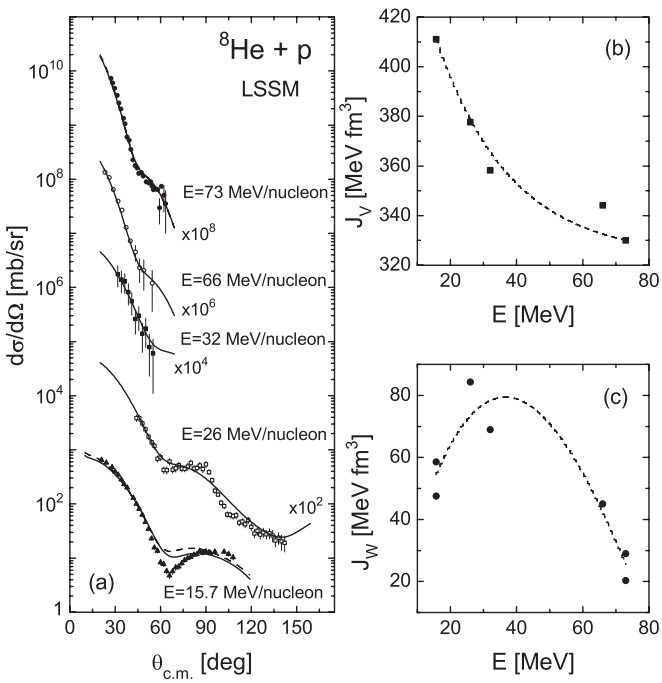

FIG. 6. The ^{8}He+p elastic-scattering cross sections (a) at different energies using LSSM density of ^{8}He and parameters from Table II. Experimental data are taken for 15.7 [12], 26 [3], 32 [10,11], 66 [10,11], and 73 MeV/nucleon [10,11,13]. The obtained values of the volume integrals J_V (b) and J_W (c) (given by points) are shown as functions of the incident energy, while the dashed lines give the trend of this dependence.

a general conception of a folding procedure. But the obtained small values of N_I and problems with the fitting of our OP at low energies deserves a special attention.

It is known that the fitting of the phenomenological OP's to the data of proton scattering on light nuclei leads to "shallow" imaginary parts of the OP's whose depths are sufficiently smaller than that of the real part of the OP. This has been observed in our previous works [40,75] for the case of ^{6}He+p elastic scattering. This is the case also in our present calculations. Another remark is connected with the difficulties in the description of the cross sections at low energies. In this case we cannot fit the data using only the volume form of OP. Instead, if one adds the contribution of a surface part of OP, then a better agreement with the data can be achieved. We note that such an admixture had been used in the earlier applications of the phenomenological OP (see, e.g., Ref. [72]).

For this reason we consider also the contribution of the surface potential:

$$U'_{\rm opt}(r) = U_{\rm opt}(r) - i4aN_S\frac{dV^F(r)}{dr}, \qquad (21)$$

where the first term in the right-hand side is the expression for the OP given by Eq. (18) [in which the ImOP is taken in the form of $V^F(r)$] and the second term is responsible for the surface effects. We note that, in particular, for the lowest incident energy, the combination of the microscopically folded real and imaginary parts in the form of V^F is more appropriate. In Eq. (21) a is the diffuseness parameter of $V^F(r)$ fitted by WS form.

We present in Fig. 7(a) our results for both the volume and all components of the imaginary part of the potential $U'_{\rm opt}(r)$ and in Fig. 7(b) for the cross section in the case of $E = 15.7$ MeV/nucleon obtained using the LSSM density of ^{8}He. The calculations are performed by fitting the strength parameters N_R, N_I, N_R^{SO}, N_I^{SO} entering Eqs. (18) and (21) and the depth parameter N_S of the surface term of the OP [Eq. (21)]. In this case $N_R = 1.078$, $N_I = 0.036$, $N_R^{SO} = N_I^{SO} = 0$, $N_S = 0.207$, $a = 0.686$ fm, $\sigma_R = 791.1$ mb. It is seen from Fig. 7 that the inclusion of the surface contribution to the imaginary part of the OP improves the agreement with the experimental data, especially for small angles and in the region of the cross-section minimum. Obviously, for more successful description of the cross sections at low energies (15.7 and 26 MeV/nucleon) our method has to be modified and improved by an inclusion of virtual excitations of inelastic and decay channels of the reactions.

From the results presented in this section one can see that a notable renormalization of the imaginary parts of the microscopic OP and the necessity of its shape correction at lower energies are needed for a reliable explanation of the data. In this connection one should note that both the folding and HEA potentials have the same physical origin, namely they are one-particle folding potentials, and thus they do not account for more complicated dynamical processes. We have already mentioned the role of the inelastic and breakup channels. In the last years many works have appeared where amplitudes of these processes were calculated within the distorted-wave approximation and also by using the coupled-channels methods. The latter also provide a way

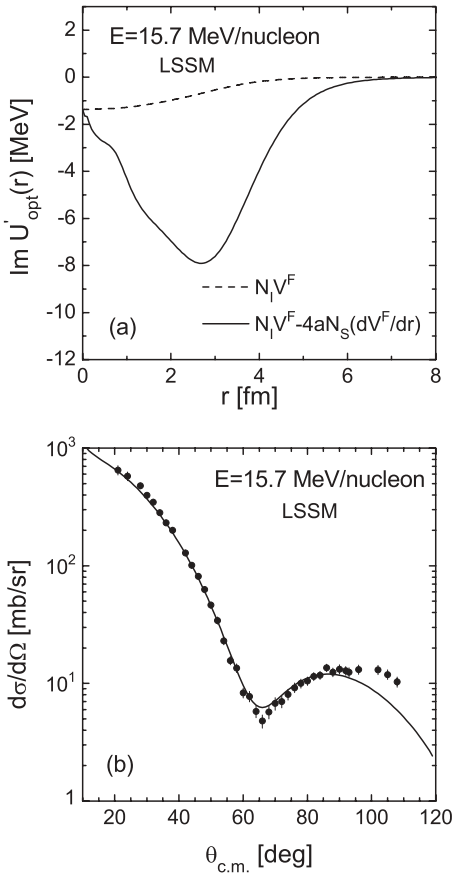

FIG. 7. (a) Volume (dashed line) and total (solid line) imaginary parts of the OP $U'_{\rm opt}(r)$ [Eq. (21)] calculated using the LSSM density of ^{8}He for energy $E = 15.7$ MeV/nucleon; (b) The ^{8}He+p elastic-scattering cross section at energy $E = 15.7$ MeV/nucleon using LSSM density of ^{8}He with fitted values of N_R, N_I, $N_R^{\rm SO}$, $N_I^{\rm SO}$, and N_S given in the text. Experimental data are taken from Ref. [12].

of estimating the elastic-scattering cross sections (see, e.g., Ref. [76] and references therein). However, if one considers the elastic channel itself, the general and formally established concept of the Feshbach theory [77] can give us a basis for the following qualitative physical suggestion. Indeed, in this theory the elastic-scattering potential is composed of two parts, the bare potential composed from one-particle matrix elements and the so-called dynamical polarization potential. Then, transforming this concept onto our model of OP, one can suppose that the bare OP is the microscopically calculated $V_{\rm sp} = V^F + iW^H$ potential having the strength $N_{R,I} \cong 1$. And the residual part of the optical potential $V_{\rm pol} \cong V_{\rm fit} - V_{\rm sp}$, being the difference between the fitted OP and $V_{\rm sp}$, may be identified with a polarization potential. In the framework of this outline of the scattering mechanism one can compare, for example, the imaginary part $W_{\rm pol}$ with the imaginary part $W_{\rm breakup}$ obtained by fitting the breakup cross sections with the respective experimental data (see, e.g., Ref. [78]) to make conclusions on the contributions of the breakup channel to the whole picture of scattering. In fact, it is seen in Fig. 7 a broad minimum of the $\mathrm{Im}U'_{\rm opt}(r)$ around $r = 2.6$ fm that illustrates qualitatively the strong effect of the breakup channel on the elastic-scattering cross section.

IV. SUMMARY AND CONCLUSIONS

The results of the present work can be summarized as follows:

(i) The optical potentials and cross sections of ^{8}He+p elastic scattering were calculated at the energies of 15.7, 26, 32, 66, and 73 MeV/nucleon and comparison with the available experimental data was performed.
  (a) The direct and exchange parts of the real OP (V^F) were calculated microscopically using the folding procedure and density-dependent M3Y (CDM3Y6-type) effective interaction based on the Paris NN potential.
  (b) The imaginary part of the OP (W^H) was calculated using the high-energy approximation.
  (c) Three different model densities of protons and neutrons in ^{8}He were used in the calculations: the Tanihata densities [47], the LSSM densities [44,45], and the densities obtained in an approach [61,62] with accounting for the central-type NN short-range Jastrow correlations.
  (d) The spin-orbit contribution to the OP was also included in the calculations.
  (e) The ^{8}He+p elastic-scattering differential cross sections and total reaction cross sections were calculated using the program DWUCK4 [68].

(ii) The density and energy dependence of the effective NN interaction were studied. It was shown that the behavior of the cross sections for given energies and interval of angles is weakly sensitive to the choice of the model for the ^{8}He density. The further calculations of the cross sections were performed using the LSSM density because it has a realistic exponential behavior in a peripheral region of the nucleus.

(iii) It was shown that the effects of the Jastrow central short-range NN correlations on the OP's and on the shape of differential cross sections are weak.

(iv) We note that the regularization of the OP's used in this work by the introduction of the fitting parameters (N's) can serve as a quantitative test of our method but not as a tool to obtain a best agreement with the experimental data. The problem of the ambiguity of the values of the parameters N_R, N_I, $N_R^{\rm SO}$, $N_I^{\rm SO}$ (that give the "depth" of each component of the OP) when the fitting procedure is applied to a limited number of experimental data is considered. It was shown that, generally, at energies $E > 20$ MeV/nucleon a good agreement with the experimental data for the differential cross sections can be achieved by varying mainly the volume part of the OP neglecting the SO contribution. A physical criterion imposed in our work on the choice of the values of the parameters N was the known behavior (e.g., Ref. [74]) of the volume integrals J_V and J_W as functions of the incident energy

in the interval $0 < E_{\rm inc} < 100$ MeV/nucleon. Another criterion is related to the values of the total cross section of scattering and reaction. However, the corresponding empirical data for these values are missing at the energy interval considered in our work.

(v) It was shown that the difficulties arising in the explanation of the ^{8}He+p cross sections at lower energies (e.g., 15.7 and 26.25 MeV/nucleon) lead to the necessity to account for the effects of the nuclear surface (and, correspondingly, of the diffuse region of the OP). For this reason we included in the cross-section calculations the surface component of the OP and applied it to the case of $E = 15.7$ MeV/nucleon. In our opinion, the account of the latter can be considered as an imitation of the breakup channel effects. A more successful explanation of the cross section at low energies could be given by inclusion of polarization contributions due to virtual excitations of inelastic and decay channels of the reactions.

ACKNOWLEDGMENTS

The work is partly supported on the basis of the Project from the Agreement for co-operation between the INRNE-BAS (Sofia) and JINR (Dubna) and from the Agreement between BAS and Aristotle University of Thessaloniki. Three of the authors (D.N.K., A.N.A., and M.K.G.) are grateful for the support of the Bulgarian Science Fund under Contract Nos. 02-285 and Φ-1501. The authors E.V.Z. and K.V.L. thank the Russian Foundation for Basic Research (Grant No. 09-01-00770) for the partial support.

[1] G. M. Ter-Akopian *et al.*, Phys. Lett. **B426**, 251 (1998).
[2] G. M. Ter-Akopian *et al.*, in *Proceedings of the Symposium on Fundamental Issues in Elementary Matter, Bad Honnef, Germany, 2000*, edited by W. Greiner (E P Systems Bt., Debrecen, 2001), p. 371.
[3] R. Wolski *et al.*, Nucl. Phys. **A701**, 29c (2002); JINR Preprint E15-98-284, Dubna, 1998; Phys. Lett. **B467**, 8 (1999); S. Stepantsov *et al.*, Phys. Lett. **B542**, 35 (2002).
[4] L. Giot *et al.*, Nucl. Phys. **A738**, 426 (2004).
[5] K. Rusek, K. W. Kemper, and R. Wolski, Phys. Rev. C **64**, 044602 (2001).
[6] V. Lapoux *et al.*, Phys. Lett. **B517**, 18 (2001).
[7] M. D. Cortina-Gil *et al.*, Nucl. Phys. **A616**, 215c (1997).
[8] A. Lagoyannis *et al.*, Phys. Lett. **B518**, 27 (2001).
[9] M. D. Cortina-Gil *et al.*, Phys. Lett. **B371**, 14 (1996).
[10] A. A. Korsheninnikov *et al.*, Nucl. Phys. **A616**, 189c (1997).
[11] A. A. Korsheninnikov *et al.*, Nucl. Phys. **A617**, 45 (1997).
[12] F. Skaza *et al.*, Phys. Lett. **B619**, 82 (2005).
[13] A. A. Korsheninnikov *et al.*, Phys. Lett. **B316**, 38 (1993).
[14] G. D. Alkhazov *et al.*, Nucl. Phys. **A712**, 269 (2002).
[15] P. Egelhof, Prog. Part. Nucl. Phys. **46**, 307 (2001).
[16] P. Egelhof, Eur. Phys. J. A **15**, 27 (2002).
[17] S. R. Neumaier *et al.*, Nucl. Phys. **A712**, 247 (2002).
[18] P. Egelhof, O. Kisselev, G. Münzenberg, S. R. Neumaier, and H. Weick, Phys. Scr. **104**, 151 (2003), and references therein.
[19] L. L. Chulkov, C. A. Bertulani, and A. A. Korsheninnikov, Nucl. Phys. **A587**, 291 (1995).
[20] M. V. Zhukov *et al.*, Phys. Rep. **231**, 151 (1993).
[21] M. V. Zhukov, A. A. Korsheninnikov, and M. H. Smedberg, Phys. Rev. C **50**, R1 (1994).
[22] M. Avrigeanu, G. S. Anagnostatos, A. N. Antonov, and J. Giapitzakis, Phys. Rev. C **62**, 017001 (2000).
[23] M. Avrigeanu, G. S. Anagnastatos, A. N. Antonov, and V. Avrigeanu, Int. J. Mod. Phys. E **11**, 249 (2002).
[24] M. Avrigeanu, A. N. Antonov, H. Lenske, and I. Stetcu, Nucl. Phys. **A693**, 616 (2001).
[25] P. J. Dortmans, K. Amos, S. Karataglidis, and S. Raynal, Phys. Rev. C **58**, 2249 (1998).
[26] S. Karataglidis, B. A. Brown, K. Amos, and P. J. Dortmans, Phys. Rev. C **55**, 2826 (1997).
[27] K. Amos, W. A. Richter, S. Karataglidis, and B. A. Brown, Phys. Rev. Lett. **96**, 032503 (2006).
[28] P. K. Deb, B. C. Clark, S. Hama, K. Amos, S. Karataglidis, and E. D. Cooper, Phys. Rev. C **72**, 014608 (2005).
[29] P. K. Deb, K. Amos, S. Karataglidis, M. B. Chadwick, and D. G. Madland, Phys. Rev. Lett. **86**, 3248 (2001).
[30] P. K. Deb and K. Amos, Phys. Rev. C **67**, 067602 (2003).
[31] K. Amos, P. J. Dortmans, H. V. von Geramb, S. Karataglidis, and J. Raynal, Adv. Nucl. Phys. **25**, 275 (2000).
[32] H. F. Arellano and M. Girod, Phys. Rev. C **76**, 034602 (2007).
[33] R. Crespo, J. A. Tostevin, and R. C. Johnson, Phys. Rev. C **51**, 3283 (1995).
[34] R. C. Johnson, J. S. Al-Khalili, and J. A. Tostevin, Phys. Rev. Lett. **79**, 2771 (1997).
[35] J. A. Christley, J. S. Al-Khalili, J. A. Tostevin, and R. C. Johnson, Nucl. Phys. **A624**, 275 (1997).
[36] R. Crespo and R. C. Johnson, Phys. Rev. C **60**, 034007 (1999).
[37] N. C. Summers, J. S. Al-Khalili, and R. C. Johnson, Phys. Rev. C **66**, 014614 (2002).
[38] J. S. Al-Khalili, R. Crespo, R. C. Johnson, A. M. Moro, and I. J. Thompson, Phys. Rev. C **75**, 024608 (2007).
[39] M. Rodríguez-Gallardo, J. M. Arias, J. Gómez-Camacho, R. C. Johnson, A. M. Moro, I. J. Thompson, and J. A. Tostevin, Eur. Phys. J. Special Topics **150**, 51 (2007).
[40] K. V. Lukyanov, V. K. Lukyanov, E. V. Zemlyanaya, A. N. Antonov, and M. K. Gaidarov, Eur. Phys. J. A **33**, 389 (2007).
[41] R. J. Satchler and W. G. Love, Phys. Rep. **55**, 183 (1979); R. J. Satchler, *Direct Nuclear Reactions* (Clarendon, Oxford, 1983).
[42] D. T. Khoa and W. von Oertzen, Phys. Lett. **B304**, 8 (1993); **B342**, 6 (1995); D. T. Khoa, W. von Oertzen, and H. G. Bohlen, Phys. Rev. C **49**, 1652 (1994); D. T. Khoa, W. von Oertzen, and A. A. Ogloblin, Nucl. Phys. **A602**, 98 (1996); Dao T. Khoa and Hoang Sy Than, Phys. Rev. C **71**, 044601 (2005); O. M. Knyaz'kov, Sov. J. Part. Nucl. **17**, 137 (1986).
[43] D. T. Khoa and G. R. Satchler, Nucl. Phys. **A668**, 3 (2000).
[44] S. Karataglidis, P. J. Dortmans, K. Amos, and C. Bennhold, Phys. Rev. C **61**, 024319 (2000).
[45] K. Amos, in *Proceedings of the 9th Conference Nuclear Reaction Mechanisms, Varenna, Italy, June 2000*, edited by E. Gadioli (Ricerca Scientifica, Milano, 2000), p. 51.
[46] N. Anantaraman, H. Toki, and G. Bertsch, Nucl. Phys. **A398**, 269 (1983).

[47] I. Tanihata, Phys. Lett. **B289**, 261 (1992), and references therein.
[48] K. V. Lukyanov, E. V. Zemlyanaya, and V. K. Lukyanov, Phys. At. Nucl. **69**, 240 (2006).
[49] P. Shukla, Phys. Rev. C **67**, 054607 (2003).
[50] R. J. Glauber, *Lectures in Theoretical Physics*, edited by W. E. Britten and L. G. Dunham (Interscience Publishers, New York, 1959), Vol. 1, p. 315.
[51] A. G. Sitenko, Ukr. Phys. J. **4**, 152 (1959).
[52] W. Czyż and L. C. Maximon, Ann. Phys. (NY) **52**, 59 (1969).
[53] R. F. Casten and B. M. Sherrill, Prog. Part. Nucl. Phys. **45**, S171 (2000).
[54] G. D. Alkhazov *et al.*, Phys. Rev. Lett. **78**, 2313 (1997).
[55] R. M. De Vries and J. C. Peng, Phys. Rev. C **22**, 1055 (1980).
[56] A. Vitturi and F. Zardi, Phys. Rev. C **36**, 1404 (1987).
[57] S. K. Charagi and S. K. Gupta, Phys. Rev. C **41**, 1610 (1990); **46**, 1982 (1992).
[58] S. K. Charagi and S. K. Gupta, Phys. Rev. C **56**, 1171 (1997).
[59] A. de Vismes, P. Roussel-Chomaz, and F. Carstoiu, Phys. Rev. C **62**, 064612 (2000).
[60] D. M. Brink and G. R. Satchler, J. Phys. G **7**, 43 (1981).
[61] S. E. Massen and H. C. Moustakidis, Phys. Rev. C **60**, 024005 (1999).
[62] C. C. Moustakidis, S. E. Massen, C. P. Panos, M. E. Grypeos, and A. N. Antonov, Phys. Rev. C **64**, 014314 (2000).
[63] D. T. Khoa, E. Khan, G. Coló, and N. Van Giai, Nucl. Phys. **A706**, 61 (2002).
[64] X. Campy and A. Bouyssy, Phys. Lett. **B73**, 263 (1978).
[65] P. Ring and P. Schuck, *The Nuclear Many-Body Problem* (Springer-Verlag, New York, 1980), p. 542.
[66] D. T. Khoa, Phys. Rev. C **63**, 034007 (2001).
[67] P. J. Karol, Phys. Rev. C **11**, 1203 (1975).
[68] P. D. Kunz and E. Rost, in *Computational Nuclear Physics*, edited by K. Langanke *et al.* (Springer-Verlag, New York, 1993), Vol. 2, p. 88.
[69] P. Shukla, arXiv:nucl-th/0112039.
[70] Cai Xiangzhow, Feng Jun, Shen Wenqing, Ma Yugang, Wang Jiansong, and Ye Wei, Phys. Rev. C **58**, 572 (1998).
[71] F. D. Becchetti, Jr. and G. W. Greenless, Phys. Rev. **182**, 1190 (1969).
[72] A. J. Koning and J. P. Delaroche, Nucl. Phys. **A713**, 231 (2003).
[73] A. N. Tikhonov and V. Y. Arsenin, *Solutions of Ill-Posed Problems* (V. H. Winston and Sons/Wiley, New York, 1977).
[74] E. A. Romanovsky *et al.*, Bull. Rus. Acad. Sci. Phys. **62**, 150 (1998).
[75] K. V. Lukyanov, E. V. Zemlyanaya, V. K. Lukyanov, A. N. Antonov, and M. K. Gaidarov, Bull. Rus. Acad. Sci. Phys. **72**, 854 (2008).
[76] A. S. Denikin, V. I. Zagrebaev, and P. Descouvemont, Phys. Rev. C **79**, 024605 (2009).
[77] H. Feshbach, Ann. Phys. (NY) **5**, 357 (1958).
[78] A. Ingemarsson, B. R. Karlsson, and R. Shyam, Phys. Rev. C **65**, 054604 (2002).